Microstructural damage of the cortico-striatal and thalamo-cortical fibers in Fabry disease: a diffusion MRI tractometry study

Sirio Cocozza[1] · Simona Schiavi[2] · Giuseppe Pontillo[1] · Matteo Battocchio[2] · Eleonora Riccio[3] · Simona Caccavallo[4] · Camilla Russo[1] · Teodolinda Di Risi[4,5] · Antonio Pisani[4] · Alessandro Daducci[2] · Arturo Brunetti[1]

Abstract

Purpose Recent evidences have suggested the possible presence of an involvement of the extrapyramidal system in Fabry disease (FD), a rare X-linked lysosomal storage disorder. We aimed to investigate the microstructural integrity of the main tracts of the cortico-striatal-thalamo-cortical loop in FD patients.

Methods Forty-seven FD patients (mean age = 42.3 ± 16.3 years, M/F = 28/21) and 49 healthy controls (mean age = 42.3 ± 13.1 years, M/F = 19/28) were enrolled in this study. Fractional anisotropy (FA), axial (AD), radial (RD), and mean diffusivity (MD) maps were computed for each subject, and connectomes were built using a standard atlas. Diffusion metrics and connectomes were then combined to carry on a diffusion MRI tractometry analysis. The main afferent and efferent pathways of the cortico-striatal-thalamo-cortical loop (namely, bundles connecting the precentral gyrus (PreCG) with the striatum and the thalamus) were evaluated.

Results We found the presence of a microstructural involvement of cortico-striatal-thalamo-cortical loop in FD patients, predominantly affecting the left side. In particular, we found significant lower mean FA values of the left cortico-striatal fibers ($p = 0.001$), coupled to higher MD ($p = 0.001$) and RD ($p < 0.001$) values, as well as higher MD ($p = 0.01$) and RD ($p = 0.01$) values at the level of the thalamo-cortical fibers.

Conclusion We confirmed the presence of an alteration of the extrapyramidal system in FD patients, in line with recent evidences suggesting the presence of brain changes as a possible reflection of the subtle motor symptoms present in this condition. Our results suggest that, along with functional changes, microstructural damage of this pathway is also present in FD patients.

Keywords Fabry disease · Magnetic resonance imaging · Brain · Tractometry

Introduction

Fabry disease (FD) is a rare X-linked lysosomal storage caused by an incomplete catabolization and subsequent intracellular accumulation of the glycosphingolipid globotriaosylceramide (Gb3), due to the defective activity of the α-galactosidase A (α-GalA) enzyme [1]. The unmetabolized glycosphingolipid therefore accumulates in different tissues, including the heart, kidney, and central nervous system (CNS), leading to the development of clinical symptoms [1]. With reference to CNS involvement, FD has been long considered to be a condition characterized only by major cerebrovascular events [2]. Nevertheless, a subclinical although significant impairment of motor functions, which occurs independently from cerebrovascular involvement, is present in FD patients, characterized by the presence of poorer fine manual dexterity, slower gait, and reduced hand speed [3].

In line with these clinical findings, recent advanced MRI studies have showed the presence of a deeper and complex brain involvement in FD patients, with particular reference to the motor system [4]. Indeed, an alteration of the corticostriatal pathway has been described in FD patients,

✉ Giuseppe Pontillo
  giuseppe.pon@gmail.com

[1] Department of Advanced Biomedical Sciences, University "Federico II", Naples, Italy

[2] Department of Computer Science, University of Verona, Verona, Italy

[3] National Research Council of Italy (IRIB CNR), Institute for Biomedical Research and Innovation, Palermo, Italy

[4] Department of Public Health, Nephrology Unit, University "Federico II", Naples, Italy

[5] CEINGE - Advanced Biotechnologies, Naples, Italy

and a reduced functional connectivity between the motor cortex and the striatum has been described in this condition [5]. An additional evidence of the involvement of the extrapyramidal pathway in FD has been demonstrated in a recent study showing the presence of susceptibility and volumetric alterations affecting two of the main relay stations of the extrapyramidal system, namely the striatum and the substantia nigra [6].

Although widespread microstructural alterations of the white matter (WM) are known to occur in FD patients, as demonstrated by different diffusion tensor imaging (DTI) studies [7–9], to date, no information about the integrity of the cortico-basal ganglia motor loop fibers is available. Given this background, the aim of this study was to evaluate the microstructural integrity of the main afferences and efferences of the motor cortices to the basal ganglia motor loop in FD patients, to investigate the possible presence of structural connectivity changes in these connections, and to expand the current knowledge about motor involvement in this condition.

Material and methods

Participants

In this retrospective cross-sectional study, part of a larger monocentric framework on the CNS involvement in FD, genetically proven patients were included along with age- and sex-comparable healthy controls (HC). For both groups, we evaluated male and female subjects without age limitations, with the following exclusion criteria: left handedness, co-existence of other systemic conditions or any addiction, history of stroke, head trauma, or any other clinical diagnosis of diseases affecting the CNS.

For all FD patients, clinical variables of systemic organ involvement were obtained from medical records and included the following: diabetes mellitus, hypertension, cardiac arrhythmia, left ventricular hypertrophy, renal failure (for estimated glomerular filtration rates < 90 mL/min), proteinuria (for scores > 150 mg/24 h), cephalalgia, and acroparesthesia.

The study was conducted in compliance with the ethical standard and approved by the "Carlo Romano" Ethics Committee for Biomedical Activities; written informed consent was obtained from all subjects according to the Declaration of Helsinki.

MRI data acquisition

All subjects underwent an MRI scan on the same 3T scanner (Trio, Siemens Medical Systems, Erlangen, Germany), equipped with an 8-channel head coil. The MRI protocol included the following sequences: (a) 3D fluid attenuated inversion recovery (FLAIR): 160 slices; TR = 6000 ms, TE = 396 ms, TI = 2200 ms; voxel size = $1.0 \times 1.0 \times 1.0$ mm^3; (b) 3D T1-weighted: 160 slices; TR = 1900 ms, TE = 3.4 ms, TI = 900 ms, flip angle = 9°, voxel size = $1.0 \times 1.0 \times 1.0$ mm^3; (c) diffusion-weighted spin echo: TR = 7400 ms, TE = 88 ms, flip angle = 90°, voxel size = $2.2 \times 2.2 \times 2.2$ mm^3 with 64 directions at b = 1000 s/mm^2 in addition to nine b = 0 s/mm^2.

MRI data analysis

For FD patients, T2-weighted hyperintense WM lesions were segmented (when present) by an observer with more than 8 years of expertise in neuroimaging data analysis, unaware of subject identity, employing a semi-automated technique (Jim 7; http://www.xinapse.com/home.php). From the segmentation procedure, lesion loads were obtained as an index of macroscopic WM damage. Furthermore, to correct for the potential impact of WM lesions in the subsequent analyses, the corresponding lesion masks were co-registered using an affine registration to the T1-weighted volumes for an in-painting procedure, as implemented in FSL, version 5.0.10 (FMRIB Software Library; http://www.fmrib.ox.ac.uk/fsl), by filling the mask with the mean signal intensity values of the surrounding normal-appearing WM.

For all subjects, the T1-weighted volumes were segmented using the standard FreeSurfer Desikan-Killiany atlas [10] which allowed to obtain a cortical parcellation of gray matter (GM) in 85 different regions of interest (ROIs). The intracranial volume (ICV) was also calculated as the sum of GM, WM, and cerebrospinal fluid volumes, in order to correct for differences in head sizes, which are known to occur in this condition [11].

DTI data were pre-processed to correct for motion and eddy currents [12]. Standard DTI metrics of fractional anisotropy (FA), axial diffusivity (AD), radial diffusivity (RD), and mean diffusivity (MD) were computed [13] using MRtrix (http://www.mrtrix.org). To perform global anatomically constrained tractography [14] (ACT), we first co-registered the T1 and DT images using FLIRT [15] (FSL, https://fsl.fmrib.ox.ac.uk) with boundary-based cost function [16]. Then, we computed the fiber orientation distribution functions [17, 18] and generated 1 million streamlines using the iFOD2 [19] tractography algorithm from which, for each subject, we built the corresponding connectome using the FreeSurfer parcellation in 85 ROIs. From the connectomes, we extracted the bundles connecting the precentral gyrus (PreCG) with the striatum (computed as caudate nucleus plus putamen) and with the thalamus, respectively, reflecting the main afferent and efferent pathways of the motor circuit within the cortico-striatal-thalamo-cortical loop [20, 21], as well as the corticospinal tract (CST) as a representation of the pyramidal system. Thus, we built a smaller connectome using only these as ROIs (three for the left and three for the right hemisphere).

Finally, DTI metrics and connectomes were combined to carry on diffusion MRI tractometry [22], which consists in assigning to each bundle a value that is obtained by taking the mean of the chosen metric along the streamlines composing the bundle.

An example of the reconstructed tracts is available in Fig. 1.

Statistical analysis

Statistical analysis was carried out using the Statistical Package for the Social Sciences package (SPSS, Version 23, IBM, Armonk, New York). Differences in terms of age and sex were tested using a two-sample t test and a chi-squared test, respectively. A general linear model (GLM) was employed to compare the two groups in terms of the diffusion MRI tractometry values derived from each DTI metric (FA, MD, AD, RD) on both hemispheres (left and right), including age, sex, and ICV as covariates, to remove the effects of potential confounding factors not related to microstructural damage. For each DTI metric, the corresponding mean value averaged over the entire WM volume was also included in the GLM as a nuisance variable, in order to correct for an index of global WM microstructural damage.

Results were considered significant for $p < 0.05$.

Results

Forty-seven FD patients and forty-nine HC were included in this study, with the two groups being not different neither for age ($p = 0.99$) nor sex ($p = 0.10$). A complete list of the demographic and clinical information of the included population is available in Table 1.

We found a diffuse microstructural damage of the entire WM highlighted by the significant difference in FA between HC and FD (0.238 ± 0.011 vs 0.233 ± 0.012, $p = 0.02$) (Table 2) (Fig. 2), along with the presence of a microstructural involvement of cortico-striatal tracts in FD patients, predominantly affecting the left side compared with the contralateral (Table 3; Fig. 3). In particular, we found a significant reduction of mean FA values of the left cortico-striatal fibers (0.43 ± 0.02 vs 0.41 ± 0.02 for HC and FD, respectively, $p = 0.001$), coupled to an increase in MD ($0.67 \times 10^{-3} \pm 0.02 \times 10^{-3}$ mm^2/s vs $0.68 \times 10^{-3} \pm 0.03 \times 10^{-3}$ mm^2/s, $p = 0.001$) and RD ($0.50 \times 10^{-3} \pm 0.02 \times 10^{-3}$ mm^2/s vs $0.52 \times 10^{-3} \pm 0.03 \times 10^{-3}$ mm^2/s, $p < 0.001$) values, while no differences emerged when AD maps were evaluated ($1.00 \times 10^{-3} \pm 0.03 \times 10^{-3}$ mm^2/s vs $1.01 \times 10^{-3} \pm 0.03 \times 10^{-3}$ mm^2/s, $p = 0.1109$). When evaluating cortico-striatal connection on the right side, a trend of reduced mean RD was found in FD patients compared with HC, not reaching the statistical significance (0.55 ± 0.03 vs 0.56 ± 0.04, $p = 0.09$), while no differences emerged for the remaining variables ($p = 0.34$, $p = 0.16$ and $p = 0.14$ for FA, MD, and AD, respectively). Similarly, the thalamo-cortical tracts showed a predominant microstructural damage in FD patients for the left side compared with the contralateral. In particular, we found a significant increase in MD ($0.67 \times 10^{-3} \pm 0.02 \times 10^{-3}$ mm^2/s vs $0.68 \times 10^{-3} \pm 0.02 \times 10^{-3}$ mm^2/s, $p = 0.01$) and RD ($0.49 \times 10^{-3} \pm 0.03 \times 10^{-3}$ mm^2/s vs $0.51 \times 10^{-3} \pm 0.03 \times 10^{-3}$ mm^2/s, $p < 0.001$) values, while no differences emerged when FA and AD maps were evaluated. None of the metrics showed significant differences in the right hemisphere.

Finally, when evaluating microstructural changes affecting the CST, a less pronounced lateralization was found, with results showing a similar pattern of involvement, although mainly bilateral (Table 3; Fig. 3).
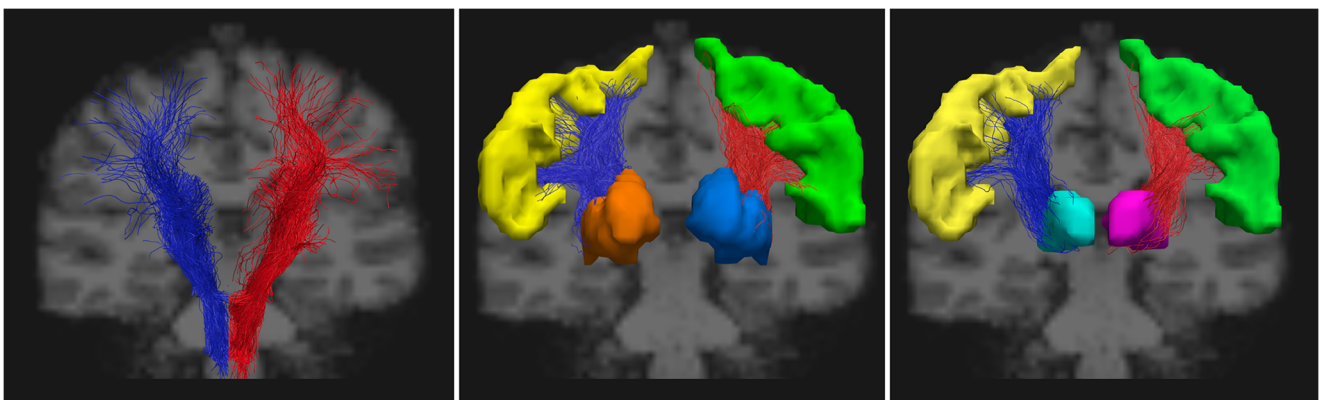

Fig. 1 Image showing the reconstructed tracts in a 29-year-old female healthy control. From left to right, the cortico-spinal, the cortico-striatal and thalamo-cortical tracts (red indicates the left side, blue the right side), with the green and yellow areas indicating the left and right precentral gyri, respectively. Finally, the dark blue and purple regions of interests represent the left striatum (as the sum of caudate nucleus and putamen) and the thalamus, while in orange and light blue are displayed the contralateral regions

Table 1 Complete list of the demographic and clinical information of the included population

	HC	FD
Age (mean ± SD)	42.3 ± 16.3	42.3 ± 13.1
Sex (M/F)	28/21	19/28
ERT	n.a.	35/47
ERT duration (mean ± SD)	n.a.	33.1 ± 30.6
Cephalalgia	n.a.	6/47
Acroparesthesia	n.a.	7/47
Hypertension	n.a.	12/47
Diabetes	n.a.	1/47
Arrhythmia	n.a.	3/47
Left ventricular hypertrophy	n.a.	23/47
Renal failure	n.a.	12/47
Proteinuria	n.a.	18/47

Subjects demographic and clinical variables of all subjects included in the study. Age is expressed in years, while ERT duration is expressed in months

FD Fabry disease, *SD* standard deviation, *ERT* enzyme replacement therapy, *n.a.* not applicable

Discussion

In FD patients, we found that prominent microstructural damage of the major WM tracts is implicated in both the extrapyramidal and pyramidal motor systems.

Poorer motor performance compared with age-matched HC has been described in FD patients, mainly involving functional domains (e.g., gait and hand speed) related to the extrapyramidal system [3]. Along with the evidence from ex vivo studies of pathologic Gb3 accumulation in different neuronal populations including the substantia nigra [23, 24], recent neuroimaging studies demonstrated the occurrence of neurodegenerative phenomena in two of the main hubs within the

Table 2 Results of the between groups analyses investigating the global WM microstructure

	HC	FD	*p*
FA	0.238 ± 0.011	0.233 ± 0.012	*0.023*
MD (10^{-3} mm^2/s)	1.032 ± 0.082	1.020 ± 0.086	0.565
AD (10^{-3} mm^2/s)	1.237 ± 0.083	1.122 ± 0.089	0.331
RD (10^{-3} mm^2/s)	0.929 ± 0.082	0.921 ± 0.086	0.711

Mean values and standard deviations of the diffusion metrics (FA, MD, AD and RD) of the entire WM for the two groups of subjects. In the last column, the *p* values obtained comparing HC and FD using a GLM with age, sex, and ICV are reported (the significant difference is in italics)

FA fractional anisotropy, *MD* mean diffusivity, *AD* axial diffusivity, *RD* radial diffusivity, *HC* healthy controls, *FD* Fabry disease, *GLM* general linear model, *ICV* intracranial volume

cortico-striatal-thalamo-cortical motor loop (i.e., striatum and substantia nigra), as well as functional disconnection between the motor cortex and the basal ganglia in this condition [5, 6]. In conjunction with these previous evidences, our results may support the hypothesis of a primary neurodegenerative damage of the extrapyramidal system, occurring at least in part independently from micro- and macro-vascular pathologies.

Indeed, microstructural damage of the cortico-striatal and thalamo-cortical projections may result from mechanisms of retrograde [25] and anterograde [26] transneuronal axonal degeneration, respectively, caused by primary neurodegeneration of intermediate relay stations—mainly the substantia nigra—within the cortico-striatal-thalamo-cortical motor loop. In accordance with this speculation, similar alterations of DTI metrics have been demonstrated in the frontal WM of Parkinson's disease (PD) patients [27–29]. On the other hand, other tractography studies on PD patients reported opposed DTI alterations (i.e., increased FA and reduced MD) of the motor cortico-striatal and thalamo-cortical tracts [30], while concordant evidences exist on the CST showing an increase of FA (and a parallel reduction of MD) associated to PD, suggesting a reorganization of these fibers possibly reflecting a compensatory increase in axonal density due to axonal sprouting [27, 31].

Furthermore, the prominent alteration of WM RD over AD showed by FD patients in our sample appears to suggest myelin damage rather than axonal degeneration [32–34], so that the observed alterations may actually reflect subtle ischemic demyelination of the investigated tracts resulting from vascular pathology [35, 36]. Indeed, a similar pattern of DTI metrics alterations is known to characterize both WM hyperintensities (WMH) and normal appearing WM (NAWM) of patients with cerebral small vessel disease (SVD) [37, 38]. In particular, several voxel-based DTI studies demonstrated that the occurrence of vascular parkinsonism is associated with more prominent microstructural damage of the bifrontal WM, the corona radiata, and the anterior limb of internal capsule, which are the main tracts involved in movement control [39–42]. Indeed, it has been hypothesized that SVD disrupts the structural integrity of WM tracts, including the corticostriatal and thalamocortical fibers, thereby reducing the influence of the basal ganglia on motor, premotor, and supplementary motor cortices [41]. This disconnection of the basal ganglia-thalamo-cortical circuit could possibly lead to subcortical atrophy, ultimately resulting in parkinsonism. Furthermore, SVD could also lower the threshold for developing parkinsonism symptoms, modifying the threshold for Lewy body pathology to become symptomatic [41]. In this light, a similar mechanism could be theorized for FD, in which widespread WM microstructural damage has been demonstrated, not sparing the major frontal WM projection tracts [7, 8], whose prominent involvement could make FD patients more prone to the development of symptomatic or even subclinical impairment of motor functional domains, mainly related to the extrapyramidal system.
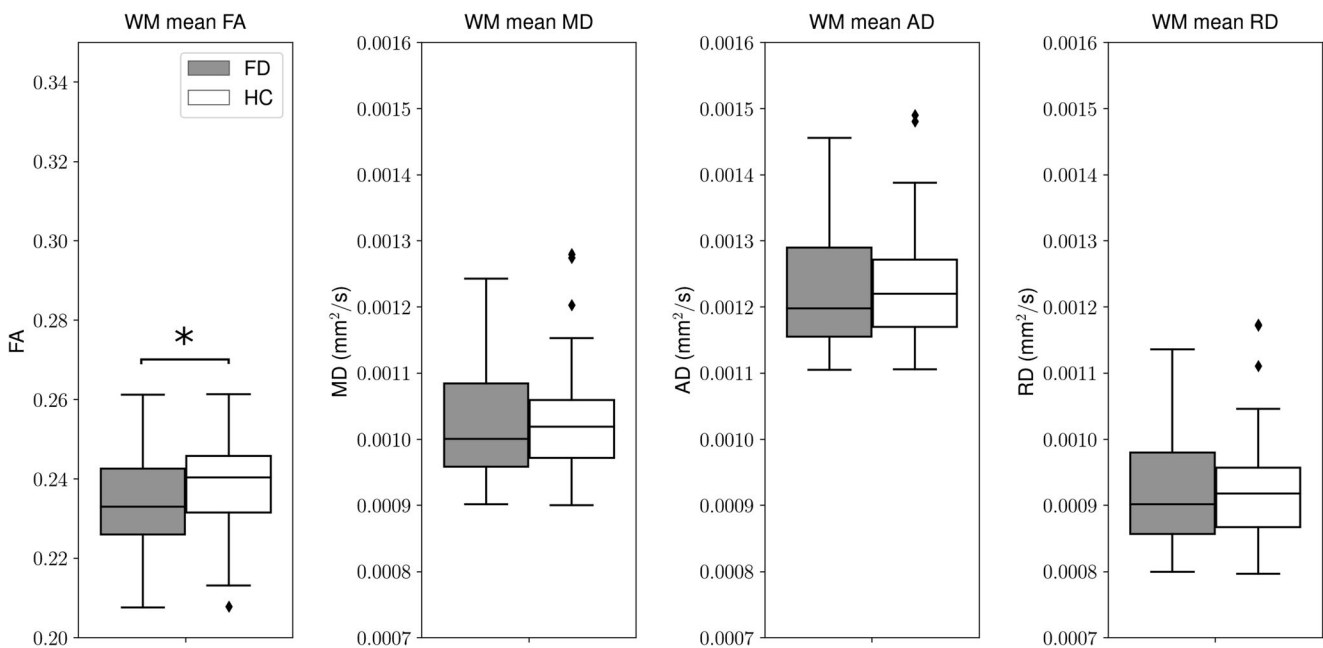
Fig. 2 Box and whiskers plot showing the differences in terms of mean microstructural values along the entire white matter in Fabry patients compared with healthy controls. Asterisk indicates significant differences between the two groups

The prominence of WM microstructural damage on the left side observed in our sample of FD patients reasonably relies on the hand dominance of the studied subjects. Indeed, an asymmetry in DTI metrics of major motor WM tracts is

Table 3 Results of the between groups analyses investigating WM microstructure along the investigated tracts

Diffusion metric	Tract	Side	HC	FD	p
FA	PrCG-striatum	R	0.413 ± 0.025	0.399 ± 0.028	0.337
		L	0.434 ± 0.024	0.412 ± 0.023	*0.005*
	Thalamus-PrCG	R	0.438 ± 0.027	0.425 ± 0.028	0.482
		L	0.462 ± 0.025	0.445 ± 0.025	0.183
	CST	R	0.499 ± 0.021	0.488 ± 0.022	0.277
		L	0.529 ± 0.021	0.510 ± 0.025	*0.037*
MD (10^{-3} mm²/s)	PrCG-striatum	R	0.723 ± 0.027	0.728 ± 0.034	0.162
		L	0.668 ± 0.019	0.685 ± 0.029	*0.001*
	Thalamus-PrCG	R	0.720 ± 0.024	0.724 ± 0.032	0.222
		L	0.669 ± 0.018	0.683 ± 0.024	*0.010*
	CST	R	0.749 ± 0.025	0.764 ± 0.026	*0.031*
		L	0.718 ± 0.026	0.740 ± 0.026	*0.002*
AD (10^{-3} mm²/s)	PrCG-striatum	R	1.065 ± 0.034	1.059 ± 0.030	0.785
		L	1.001 ± 0.037	1.006 ± 0.035	0.092
	Thalamus-PrCG	R	1.087 ± 0.035	1.080 ± 0.029	0.813
		L	1.030 ± 0.035	1.036 ± 0.030	0.089
	CST	R	1.202 ± 0.037	1.209 ± 0.034	0.307
		L	1.190 ± 0.044	1.200 ± 0.037	0.198
RD (10^{-3} mm²/s)	PrCG-striatum	R	0.551 ± 0.030	0.563 ± 0.040	0.098
		L	0.501 ± 0.021	0.525 ± 0.038	*0.0002*
	Thalamus-PrCG	R	0.536 ± 0.029	0.547 ± 0.039	0.169
		L	0.489 ± 0.021	0.507 ± 0.031	*0.014*
	CST	R	0.523 ± 0.027	0.541 ± 0.033	*0.018*
		L	0.483 ± 0.026	0.510 ± 0.031	*0.0004*

Mean values and standard deviations of the diffusion metrics (FA, MD, AD and RD) of the three WM tracts (PrCG-striatum, thalamus-PrCG, and CST) for the two groups of subjects. The *p* values obtained comparing HC and FD using a GLM with age, sex, ICV, and mean values of the metric in the entire WM are reported in the last column (significant differences are in italics)

FA fractional anisotropy, *MD* mean diffusivity, *AD* axial diffusivity, *RD* radial diffusivity, *HC* healthy controls, *FD* Fabry disease, *PrCG* precentral gyrus, *CST* cortico-spinal tract, *WM* white matter, *GLM* generalized linear model, *ICV* intracranial volume
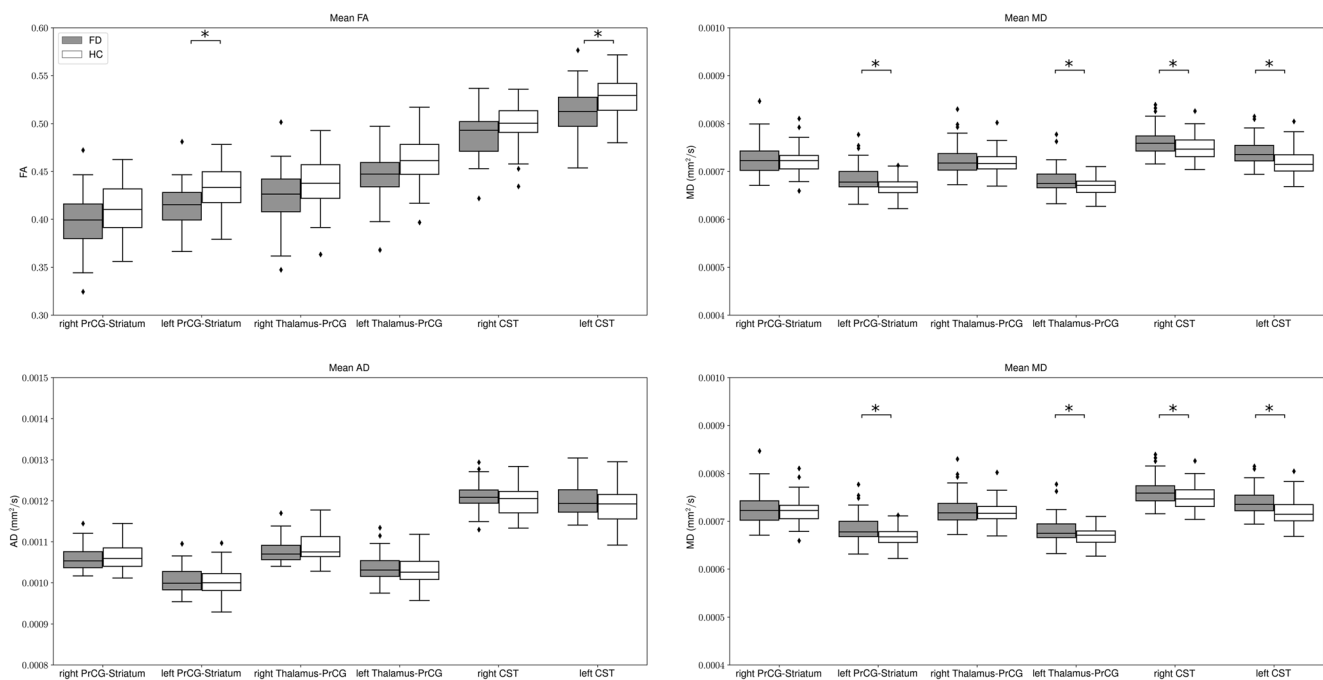
Fig. 3 Box and whiskers plot showing the results of the tractometry analyses, with mean diffusion metrics along the evaluated tracts in Fabry patients compared with healthy controls. Asterisk indicates significant differences between the two groups

known to exist in HC, with higher anisotropy values in the dominant hemisphere [43–46]. Therefore, in a condition in which a widespread microstructural damage occurs, differences of DTI metrics are more likely to emerge on the dominant side. Furthermore, due to the higher level of activation and energy demand, motor WM tracts of the dominant hemisphere are theoretically more disposed to ischemic injury and excitotoxic mechanisms [47]. Nevertheless, future studies comparing right- and left-handed FD subjects, although challenging to perform given the relatively rarity of the disease and the percentage of left-handedness in the population [48], are warranted.

Whatever its origin, disruption of the cortico-striatal projection fibers may underlie the reduction of functional connectivity between the motor cortex and the basal ganglia observed in this condition [5]. Nevertheless, it is known that the relationship between structural and functional connectivity may not be straightforward, so that future dynamic effective connectivity resting-state fMRI studies are warranted in order to unravel the causal connection between motor cortex and striatum functional activation [49].

Based on these observations, the question remains as to in which proportion primary neurodegenerative phenomena and cerebrovascular damage contribute to the motor functional impairment observed in FD. To disentangle this issue, further studies are needed, possibly oriented toward the direct investigation of microstructural damage at the level of substantia nigra and nigrostriatal connections, whose alterations bear the potential to represent more specific markers of primary neurodegenerative parkinsonism [50–54]. Furthermore, the lack of clinical data also

needs to be acknowledged as a limitation of our study. However, even if theoretically the correlation with clinical measures of motor impairment could have helped to elucidate the functional meaning of the observed WM alterations, it is known that neurological alterations in FD patients are mild [3] and thus hardly relate to findings of advanced brain MRI techniques [5, 6].

Although characterized by these limitations, our results confirm the presence of an extrapyramidal involvement in FD patients, showing the presence of microstructural changes significantly affecting the cortico-striatal pathway in this condition, further confirming the presence of a deep and complex involvement of motor circuits in FD.

Compliance with ethical standards

Conflict of interest S.C. received fees for speaking from Genzyme and Shire and fees for adv.board from Amicus.

Ethical approval All procedures performed in the studies involving human participants were in accordance with the ethical standards of the institutional and/or national research committee and with the 1964 Helsinki Declaration and its later amendments or comparable ethical standards.

Informed consent Informed consent was obtained from all individual participants included in the study.

References

1. Germain DP (2010) Fabry disease. Orphanet J Rare Dis 5:30. https://doi.org/10.1186/1750-1172-5-30

2. Kolodny E, Fellgiebel A, Hilz MJ, Sims K, Caruso P, Phan TG, Politei J, Manara R, Burlina A (2015) Cerebrovascular involvement in Fabry disease: current status of knowledge. Stroke 46(1):302–313. https://doi.org/10.1161/STROKEAHA.114.006283

3. Lohle M, Hughes D, Milligan A, Richfield L, Reichmann H, Mehta A, Schapira AH (2015) Clinical prodromes of neurodegeneration in Anderson-Fabry disease. Neurology 84(14):1454–1464. https://doi.org/10.1212/WNL.0000000000001450

4. Cocozza S, Russo C, Pontillo G, Pisani A, Brunetti A (2018) Neuroimaging in Fabry disease: current knowledge and future directions. Insights Imaging 9(6):1077–1088. https://doi.org/10.1007/s13244-018-0664-8

5. Cocozza S, Pisani A, Olivo G, Sacca F, Ugga L, Riccio E, Migliaccio S, Brescia Morra V, Brunetti A, Quarantelli M, Tedeschi E (2017) Alterations of functional connectivity of the motor cortex in Fabry disease: an RS-fMRI study. Neurology 88(19):1822–1829. https://doi.org/10.1212/WNL.0000000000003913

6. Russo C, Pontillo G, Pisani A, Sacca F, Riccio E, Macera A, Rusconi G, Stanzione A, Borrelli P, Brescia Morra V, Tedeschi E, Brunetti A, Cocozza S, Palma G (2018) Striatonigral involvement in Fabry disease: a quantitative and volumetric magnetic resonance imaging study. Parkinsonism Relat Disord 57:27–32. https://doi.org/10.1016/j.parkreldis.2018.07.011

7. Albrecht J, Dellani PR, Muller MJ, Schermuly I, Beck M, Stoeter P, Gerhard A, Fellgiebel A (2007) Voxel based analyses of diffusion tensor imaging in Fabry disease. J Neurol Neurosurg Psychiatry 78(9):964–969. https://doi.org/10.1136/jnnp.2006.112987

8. Cocozza S, Pontillo G, Quarantelli M, Sacca F, Riccio E, Costabile T, Olivo G, Brescia Morra V, Pisani A, Brunetti A, Tedeschi E (2018) Default mode network modifications in Fabry disease: a resting-state fMRI study with structural correlations. Hum Brain Mapp 39(4):1755–1764. https://doi.org/10.1002/hbm.23949

9. Paavilainen T, Lepomaki V, Saunavaara J, Borra R, Nuutila P, Kantola I, Parkkola R (2013) Diffusion tensor imaging and brain volumetry in Fabry disease patients. Neuroradiology 55(5):551–558. https://doi.org/10.1007/s00234-012-1131-8

10. Desikan RS, Segonne F, Fischl B, Quinn BT, Dickerson BC, Blacker D, Buckner RL, Dale AM, Maguire RP, Hyman BT, Albert MS, Killiany RJ (2006) An automated labeling system for subdividing the human cerebral cortex on MRI scans into gyral based regions of interest. NeuroImage 31(3):968–980. https://doi.org/10.1016/j.neuroimage.2006.01.021

11. Pontillo G, Cocozza S, Brunetti A, Brescia Morra V, Riccio E, Russo C, Sacca F, Tedeschi E, Pisani A, Quarantelli M (2018) Reduced intracranial volume in Fabry disease: evidence of abnormal neurodevelopment? Front Neurol 9:672. https://doi.org/10.3389/fneur.2018.00672

12. Andersson JLR, Sotiropoulos SN (2016) An integrated approach to correction for off-resonance effects and subject movement in diffusion MR imaging. NeuroImage 125:1063–1078. https://doi.org/10.1016/j.neuroimage.2015.10.019

13. Veraart J, Sijbers J, Sunaert S, Leemans A, Jeurissen B (2013) Weighted linear least squares estimation of diffusion MRI parameters: strengths, limitations, and pitfalls. NeuroImage 81:335–346. https://doi.org/10.1016/j.neuroimage.2013.05.028

14. Smith RE, Tournier JD, Calamante F, Connelly A (2012) Anatomically-constrained tractography: improved diffusion MRI streamlines tractography through effective use of anatomical information. NeuroImage 62(3):1924–1938. https://doi.org/10.1016/j.neuroimage.2012.06.005

15. Jenkinson M, Bannister P, Brady M, Smith S (2002) Improved optimization for the robust and accurate linear registration and motion correction of brain images. NeuroImage 17(2):825–841. https://doi.org/10.1016/s1053-8119(02)91132-8

16. Greve DN, Fischl B (2009) Accurate and robust brain image alignment using boundary-based registration. NeuroImage 48(1):63–72. https://doi.org/10.1016/j.neuroimage.2009.06.060

17. Tournier JD, Calamante F, Connelly A (2007) Robust determination of the fibre orientation distribution in diffusion MRI: non-negativity constrained super-resolved spherical deconvolution. NeuroImage 35(4):1459–1472. https://doi.org/10.1016/j.neuroimage.2007.02.016

18. Tournier JD, Calamante F, Connelly A (2013) Determination of the appropriate b value and number of gradient directions for high-angular-resolution diffusion-weighted imaging. NMR Biomed 26(12):1775–1786. https://doi.org/10.1002/nbm.3017

19. Tournier JDC, Connelly F (2010) A improved probabilistic streamlines tractography by 2nd order integration over fibre orientation distributions. In: ISMRM

20. Lanciego JL, Luquin N, Obeso JA (2012) Functional neuroanatomy of the basal ganglia. Cold Spring Harb Perspect Med 2(12): a009621. https://doi.org/10.1101/cshperspect.a009621

21. Obeso JA, Rodriguez-Oroz MC, Benitez-Temino B, Blesa FJ, Guridi J, Marin C, Rodriguez M (2008) Functional organization of the basal ganglia: therapeutic implications for Parkinson's disease. Mov Disord 23(Suppl 3):S548–S559. https://doi.org/10.1002/mds.22062

22. Bells S, Cercignani M, Deoni S, Assaf Y, Pasternak O, Evans CJ, Leemans A, Jones DK (2011) Tractometry–comprehensive multimodal quantitative assessment of white matter along specific tracts. In: Proc. Intl. Soc. Mag. Reson. Med., vol 19

23. deVeber GA, Schwarting GA, Kolodny EH, Kowall NW (1992) Fabry disease: immunocytochemical characterization of neuronal involvement. Ann Neurol 31(4):409–415. https://doi.org/10.1002/ana.410310410

24. Kaye EM, Kolodny EH, Logigian EL, Ullman MD (1988) Nervous system involvement in Fabry's disease: clinicopathological and biochemical correlation. Ann Neurol 23(5):505–509. https://doi.org/10.1002/ana.410230513

25. Patel KR, Ramsey LE, Metcalf NV, Shulman GL, Corbetta M (2016) Early diffusion evidence of retrograde transsynaptic degeneration in the human visual system. Neurology 87(2):198–205. https://doi.org/10.1212/WNL.0000000000002841

26. Kanamori A, Catrinescu MM, Belisle JM, Costantino S, Levin LA (2012) Retrograde and Wallerian axonal degeneration occur synchronously after retinal ganglion cell axotomy. Am J Pathol 181(1): 62–73. https://doi.org/10.1016/j.ajpath.2012.03.030

27. Atkinson-Clement C, Pinto S, Eusebio A, Coulon O (2017) Diffusion tensor imaging in Parkinson's disease: review and meta-analysis. NeuroImage Clinical 16:98–110. https://doi.org/10.1016/j.nicl.2017.07.011

28. Cochrane CJ, Ebmeier KP (2013) Diffusion tensor imaging in parkinsonian syndromes: a systematic review and meta-analysis.

Neurology 80(9):857–864. https://doi.org/10.1212/WNL.0b013e318284070c

29. Planetta PJ, McFarland NR, Okun MS, Vaillancourt DE (2014) MRI reveals brain abnormalities in drug-naive Parkinson's disease. Exerc Sport Sci Rev 42(1):12–22. https://doi.org/10.1249/JES.0000000000000003

30. Mole JP, Subramanian L, Bracht T, Morris H, Metzler-Baddeley C, Linden DE (2016) Increased fractional anisotropy in the motor tracts of Parkinson's disease suggests compensatory neuroplasticity or selective neurodegeneration. Eur Radiol 26(10):3327–3335. https://doi.org/10.1007/s00330-015-4178-1

31. Arkadir D, Bergman H, Fahn S (2014) Redundant dopaminergic activity may enable compensatory axonal sprouting in Parkinson disease. Neurology 82(12):1093–1098. https://doi.org/10.1212/WNL.0000000000000243

32. Alexander AL, Lee JE, Lazar M, Field AS (2007) Diffusion tensor imaging of the brain. Neurotherapeutics 4(3):316–329. https://doi.org/10.1016/j.nurt.2007.05.011

33. Aung WY, Mar S, Benzinger TL (2013) Diffusion tensor MRI as a biomarker in axonal and myelin damage. Imaging Med 5(5):427–440. https://doi.org/10.2217/iim.13.49

34. Winklewski PJ, Sabisz A, Naumczyk P, Jodzio K, Szurowska E, Szarmach A (2018) Understanding the physiopathology behind axial and radial diffusivity changes-what do we know? Front Neurol 9:92. https://doi.org/10.3389/fneur.2018.00092

35. Kelley RE (2006) Ischemic demyelination. Neurol Res 28(3):334–340. https://doi.org/10.1179/016164106X98242

36. Shi Y, Wardlaw JM (2016) Update on cerebral small vessel disease: a dynamic whole-brain disease. Stroke Vasc Neurol 1(3):83–92. https://doi.org/10.1136/svn-2016-000035

37. Pasi M, van Uden IW, Tuladhar AM, de Leeuw FE, Pantoni L (2016) White matter microstructural damage on diffusion tensor imaging in cerebral small vessel disease: clinical consequences. Stroke 47(6):1679–1684. https://doi.org/10.1161/STROKEAHA.115.012065

38. Raja R, Rosenberg G, Caprihan A (2019) Review of diffusion MRI studies in chronic white matter diseases. Neurosci Lett 694:198–207. https://doi.org/10.1016/j.neulet.2018.12.007

39. Deverdun J, Menjot de Champfleur S, Cabello-Aguilar S, Maury F, Molino F, Charif M, Leboucq N, Ayrignac X, Labauge P, Bonafe A, Castelnovo G, Le Bars E, Geny C, Menjot de Champfleur N (2014) Diffusion tensor imaging differentiates vascular parkinsonism from parkinsonian syndromes of degenerative origin in elderly subjects. Eur J Radiol 83(11):2074–2079. https://doi.org/10.1016/j.ejrad.2014.07.012

40. Salsone M, Caligiuri ME, Vescio V, Arabia G, Cherubini A, Nicoletti G, Morelli M, Quattrone A, Vescio B, Nistico R, Novellino F, Cascini GL, Sabatini U, Montilla M, Rektor I, Quattrone A (2019) Microstructural changes of normal-appearing white matter in vascular parkinsonism. Parkinsonism Relat Disord 63:60–65. https://doi.org/10.1016/j.parkreldis.2019.02.046

41. van der Holst HM, van Uden IW, Tuladhar AM, de Laat KF, van Norden AG, Norris DG, van Dijk EJ, Esselink RA, Platel B, de Leeuw FE (2015) Cerebral small vessel disease and incident parkinsonism: the RUN DMC study. Neurology 85(18):1569–1577. https://doi.org/10.1212/WNL.0000000000002082

42. Wang HC, Hsu JL, Leemans A (2012) Diffusion tensor imaging of vascular parkinsonism: structural changes in cerebral white matter and the association with clinical severity. Arch Neurol 69(10):1340–1348. https://doi.org/10.1001/archneurol.2012.633

43. Angstmann S, Madsen KS, Skimminge A, Jernigan TL, Baare WF, Siebner HR (2016) Microstructural asymmetry of the corticospinal tracts predicts right-left differences in circle drawing skill in right-handed adolescents. Brain Struct Funct 221(9):4475–4489. https://doi.org/10.1007/s00429-015-1178-5

44. Catani M, Forkel SJ, Thiebaut De Schotten M (2010) Asymmetry of white matter pathways. In: Hugdahl K, Westerhausen R (eds) The two halves of the brain: information processing in the cerebral hemispheres. MIT Press, Cambridge, pp 177–210

45. Nathan PW, Smith MC, Deacon P (1990) The corticospinal tracts in man. Course and location of fibres at different segmental levels. Brain J Neurol 113(Pt 2):303–324. https://doi.org/10.1093/brain/113.2.303

46. Trivedi R, Agarwal S, Rathore RK, Saksena S, Tripathi RP, Malik GK, Pandey CM, Gupta RK (2009) Understanding development and lateralization of major cerebral fiber bundles in pediatric population through quantitative diffusion tensor tractography. Pediatr Res 66(6):636–641. https://doi.org/10.1203/PDR.0b013e3181bbc6b5

47. Tekkok SB, Ye Z, Ransom BR (2007) Excitotoxic mechanisms of ischemic injury in myelinated white matter. J Cereb Blood Flow Metab 27(9):1540–1552. https://doi.org/10.1038/sj.jcbfm.9600455

48. Papadatou-Pastou M, Ntolka E, Schmitz J, Martin M, Munafo MR, Ocklenburg S, Paracchini S (2020) Human handedness: a meta-analysis. Psychol Bull 146(6):481–524. https://doi.org/10.1037/bul0000229

49. Park HJ, Friston KJ, Pae C, Park B, Razi A (2018) Dynamic effective connectivity in resting state fMRI. NeuroImage 180(Pt B):594–608. https://doi.org/10.1016/j.neuroimage.2017.11.033

50. Deng XY, Wang L, Yang TT, Li R, Yu G (2018) A meta-analysis of diffusion tensor imaging of substantia nigra in patients with Parkinson's disease. Sci Rep 8(1):2941. https://doi.org/10.1038/s41598-018-20076-y

51. Langley J, Huddleston DE, Merritt M, Chen X, McMurray R, Silver M, Factor SA, Hu X (2016) Diffusion tensor imaging of the substantia nigra in Parkinson's disease revisited. Hum Brain Mapp 37(7):2547–2556. https://doi.org/10.1002/hbm.23192

52. Tan WQ, Yeoh CS, Rumpel H, Nadkarni N, Lye WK, Tan EK, Chan LL (2015) Deterministic tractography of the nigrostriatal-nigropallidal pathway in Parkinson's disease. Sci Rep 5:17283. https://doi.org/10.1038/srep17283

53. Theisen F, Leda R, Pozorski V, Oh JM, Adluru N, Wong R, Okonkwo O, Dean DC 3rd, Bendlin BB, Johnson SC, Alexander AL, Gallagher CL (2017) Evaluation of striatonigral connectivity using probabilistic tractography in Parkinson's disease. NeuroImage Clinical 16:557–563. https://doi.org/10.1016/j.nicl.2017.09.009

54. Zhang Y, Wu IW, Buckley S, Coffey CS, Foster E, Mendick S, Seibyl J, Schuff N (2015) Diffusion tensor imaging of the nigrostriatal fibers in Parkinson's disease. Mov Disord 30(9):1229–1236. https://doi.org/10.1002/mds.26251